Available online at www.sciencedirect.com

SCIENCE DIRECT®

Talanta 68 (2006) 1322–1328

Talanta

www.elsevier.com/locate/talanta

Fabrication of nanometre-sized platinum electrodes by controllable electrochemical deposition

Chengyin Wang, Xiaoya Hu [*]

College of Chemistry and Chemical Engineering, Yangzhou University, Yangzhou 225002, China

Received 2 February 2005; received in revised form 21 July 2005; accepted 23 July 2005

Abstract

A new and simple method for fabricating controllable insulated nanometer-sized platinum electrodes is presented. Electrochemical etching of platinum wire is employed, and then a repeated process of cycle voltammetric deposition of electrophoretic paint and heat curing for shrink film follows which effectively controls the size of the nanoelectrodes, which is different from previous DC electrolysis deposition. This technique allows complete insulation of the whole body of the etched platinum wire, except for the very tip with the shrink film during heat curing of the film, leaving an electrochemical active area with effective diameters of nanometers. The process overcomes the pinhole formation resulting from the electrophoretic paint deposition process. The size of the platinum electrodes and the thickness of the deposed paint for insulation can be properly controlled and reproduced. The fabricated electrodes show ideal steady-state voltammetric behaviors from which the effective areas of the nanoelectrodes are measured. The effective radius of the prepared nanoelectrodes ranges from 3.1 nm to hundreds of nanometers.

Keywords: Platinum electrode; Electrophoretic paint; Nanoelectrode

1. Introduction

Nanoelectrodes have evoked comprehensive interest due to their intrinsic characteristics. The low *iR* drop enables a two-electrode system to be used and the high-resistance system to be detected. The low charged currents of the nanoelectrodes increase the ratio of signal/noise and allow a high scan rate. In addition, a decrease in electrode dimensions has allowed measurements to be made in the live organism [1–5]. One of the greatest challenges facing nanoelectrode researchers is the preparation and fabrication of devices in order to study and realize some of the benefits discussed above. This aspect has been the most studied topic in this area over the last 15 years or so. Several research groups have reported fabrication of platinum electrodes having electrochemically active radii as small as several hundred nanometers, and even down to a few tens of nanometers [6–10]. Platinum micro-band electrodes have been produced with a dimension less than 20 nm [11].

Unwin and co-workers [12] introduced the use of electrophoretically-deposited paints to insulate the tip. Either cathodic or anodic deposition of paints can be employed. Post-painting heat treatment is required in order to shrink the paint and force the tip of the etched metal cone to protrude. This approach has been taken up by others [13,14] as well as subjected to further improvements in the painting procedure [15]. This approach enables some really small electrodes to be manufactured (sub-nm up to hundreds of nanometers) and is presently the most widely used approach to achieve ultra-small electrodes on a one-off basis for fundamental studies [16]. The size of the coating is controllable by the number of electrophoretic painting/heat treatment cycles used: the more painting/heat treatments, the smaller the apparent nanoelectrode dimensions. It is also low cost, using an apparatus that is commonly available in electrochemistry laboratories. All that is needed other than a regular electrochemical apparatus is an AC voltage supply. Although the platinum electrodes

---

[*] Corresponding author. Tel.: +86 514 7975587; fax: +86 514 7975244.
E-mail address: xyhu@yzu.edu.cn (X. Hu).

0039-9140/$ – see front matter © 2005 Elsevier B.V. All rights reserved.
doi:10.1016/j.talanta.2005.07.048

with electroactive radii ranged from 1 μm to 10 nm have been fabricated, the size of the platinum electrodes and the thickness of the deposed paint for insulation can not be reliably controlled reproducibly.

This paper describes a simple, inexpensive and highly effective method for producing controllable platinum electrodes with dimensions in the range of 3.1 nm to hundreds of nanometers by a repeated process of cycle voltammetric depositing the electrophoretic paint and heating the film for exposing the tip of the electrode. The process overcomes pinhole formation resulted from the electrophoretic paint deposition process. The size of the platinum electrodes and the thickness of the deposed paint for insulation can be probably controlled reproducibly. The fabricated electrodes have ideal steady-state voltammetric behaviors from which the effective areas of the nanoelectrodes are measured.

2. Experimental

2.1. Instruments and chemicals

All electrochemical measurements were performed on an electrochemical workstation with the ECD (CHI 660A, Chenhua Instrument Limited Company, Shanghai) in conjunction with a computer. The high-sensitivity preamplifier (1 pA/V) of the potentiostat was used in all of the experiments. A three-electrode system was employed. A nanometer-sized wire electrode was used as a working electrode. A saturated calomel electrode and a platinum plate served, respectively, as the reference and auxiliary electrodes.

A scanning electron microscope (XL-30 ESEM, Philips, Holland) was used for surface examination of the etched electrodes. Platinum wires with a radius of 10 μm were purchased from Shanghai Chemicals Corp. of China. Anodic electrophoretic paint was purchased from Taixing Chemical Plant of China. Other reagents used in this work were analytical grade. Water used in the experiment was double distilled water.

2.2. Electrochemical etching of platinum wire

In a typical experiment [13], a platinum wire of about 10 mm in length was attached to one end of a copper wire with a spot welding. The copper–platinum wire was mounted on a micromanipulator (Fig. 1). After being rinsed with ethanol and water, the wire was gently transferred into the etching solution (saturated sodium nitrite solution). An AC voltage was applied between the wire and a platinum foil electrode. After being etched, the wire was rinsed with water to remove residual $NaNO_2$.

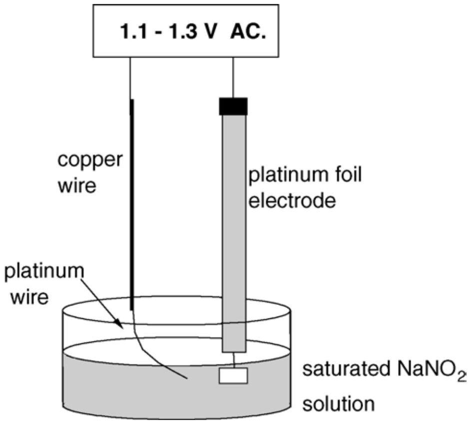

Fig. 1. The schematics of the etching of platinum wire.

2.3. The electrophoretic paint insulation of the etched platinum wire

The etched platinum wire was inserted into the glass capillary with the tip of the platinum wire kept outside of the glass capillary. The two ends of the assembled glass electrode were sealed with an epoxy resin. The configuration of the platinum wire cone electrode is depicted in Fig. 2.

Insulation of the etched Pt wire was accomplished using an anodic electrophoretic paint. The paint consists of poly (acrylic acid) (PAAH) with an excess of base added in order to deprotonate the acid groups, yielding a water-soluble species (PAA^-). The exposed portion of the Pt wire was completely immersed in a diluted aqueous paint solution (20:1) and positioned in the center of a Pt coil (∼1-cm diameter) so as to increase the infiltrativity of the electrophoretic paint [17]. In this case, the cycle voltammetry in the solution with three-electrode system was employed to deposit the anodic electrophoretic paint on the etched platinum cone electrode. The scan potentials ranged from +1.0 V to 2.2 V to initiate the oxidation of water [15].

$$2H_2O \rightarrow O_2 + 4H^+ + 4e^- \quad (1)$$

The local change in the pH at the electrode surface shifts the equilibrium to the protonated species, PAAH:

$$PAA^- + H^+ \rightarrow PAAH \quad (2)$$

which is water insoluble and adsorbs onto the Pt surface. After deposition, spray rinsing was used to remove any loose solution from the wire. The platinum wire was then heated at 130 °C for about 15 min to let the deposited film cure. Nanometer-sized electrodes were obtained by applying multiple depositions and cures of PAAH. Electrodes can be reused and have lifespans of a few weeks depending on the amount of usage.

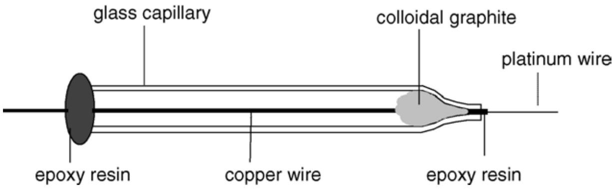

Fig. 2. The schematics of the etched platinum nanoelectrode.

2.4. Determination of the effective radius of the nanoelectrodes

The effective radius and the geometric areas of the nanoelectrodes were determined by the limiting plateau current of the cycle voltammetry in 0.01 mol/L $K_3Fe(CN)_6$ solution containing 0.5 mol/L KCl. A saturated calomel electrode and a platinum plate served, respectively, as the reference and auxiliary electrode. The scan rate was 5 mV/s.

3. Results and discussion

3.1. Effect of the etching voltage

The voltage employed for the electrochemical process affects the shape of the etched platinum wire tip. When the voltage is equal to or larger than 1.1 V, the etching process becomes too fast within several seconds and the tip shows an irregular shape. The SEM image of the etched platinum wire is shown in Fig. 3(a). When the voltage is in the range of 1.1–1.3 V, the peaked tip is obtained (Fig. 3(b) and (c)). When the voltage is less than 1.3 V, more than 1 h is spent. So the etching voltage of 1.1–1.3 V was chosen. Additionally, the Pt wire was etched to a sharp point by placing the wire in a saturated sodium nitrite solution. The sharpest point of the etched Pt wire was obtained when the end of Pt wire was inclined to be submerged in the electrochemical etching solution at a 30–60° angle rather than submerged perpendicularly (Fig. 1).

3.2. Effect of the concentration of sodium nitrite solution

The concentration of the sodium nitrite solution also plays an important role in the shape of the etched platinum wire tip and the etching time. When the concentration of sodium nitrite solution is less than 1 mol/L, the etching rate is slow; the surface of the etched platinum wire tip is rough, and the tip is easily broken. By increasing the concentration of the sodium nitrite solution, the etching is quicker, and the tip becomes sharp enough. Therefore, a saturated sodium nitrite solution was the best choice for etching platinum wire.

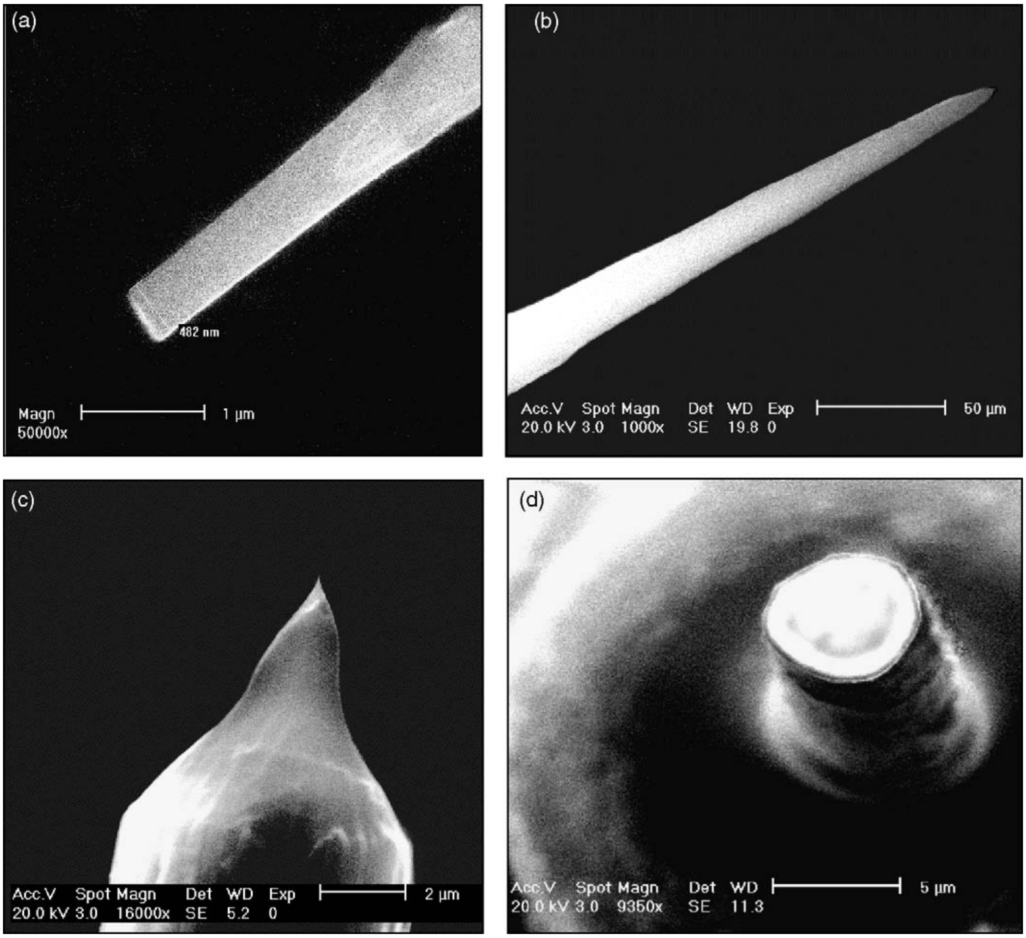

Fig. 3. Scanning electron microscopy images of the etched nanoelectrodes with different voltages (a) low 1.1 V; (b) 1.1–1.3 V; (c) is the image which is magnified from (b). The concentration of the sodium nitrite: saturated solution; (d) the section plane of an un-etched platinum wire electrode after the third deposition/coating. The thickness of the insulating sheath is about 200 nm.

3.3. Insulation of the etched platinum wire

The cathodic electrophoretic paint was deposited on the platinum cone electrode by using the cyclic voltammetry from 1.0 V to 2.2 V with a scan rate of 5 mV/s. The current of the cyclic voltammetry drops gradually with the increase of consecutive scan times. Fig. 4(A) shows voltammograms of the electrophoretic paint being gradually deposited, and the currents tend to be constant after the number of cycles is increased to about 20. Then the electrode is coated with the insulated film. The film shrinkage during the heat curing procedure of the film leaves only the end of the tip exposed. Fig. 3(d) shows the section plane of an un-etched platinum wire electrode after the third deposition/coating and the thickness of the insulating sheath is about 200 nm. The steady-state voltammogram (Fig. 4(B)) in the $K_3Fe(CN)_6$ solution is obtained after the first deposition due to the retraction of the film from the tip end. The effective radius is 994 nm. However, the exposed tip is hundreds of nanometer during the above procedure only for once. Repeating the coating and curing procedure will achieve the desired nanoelectrode dimensions. The voltammograms of the sixth deposition are shown in Fig. 4(C). Fig. 4(D) shows the steady-state voltammograms in the $K_3Fe(CN)_6$ solution after the sixth deposition. The effective radius is reduced to 3.1 nm. Therefore, a smaller-sized nanoelectrode can be produced by increasing the number of depositions of electrophoretic paint.

3.4. Characterization of nanoelectrode size and steady-state voltammetric behaviors

In characterization studies of UMEs, steady-state voltammetry (SSV) can provide an estimate of the exposed electroactive radius of the nanoelectrode [18]. Fig. 4 shows voltammograms of two platinum wire electrodes in 0.01 mol/L $K_3Fe(CN)_6$ with a supporting electrolyte of 0.5 mol/L KCl. Assuming that the electrode is a hemispherical shape, the effective radii r_{eff} of these electrodes can be determined from the limiting plateau currents (i_{lim}) according to the following equation [19]:

$$i_{\mathrm{lim}} = 2\pi n F D c r_{\mathrm{eff}} \tag{3}$$

where n is the number of electrons transferred during the electrochemical process, F is faraday's constant, while D and c are the diffusion coefficient and concentration of the electroactive species, respectively. By using the known value of the diffusion coefficient of ferricyanide, $7.2 \times 10^{-6}\ \mathrm{cm}^2/\mathrm{s}$ [20], the effective radii of the electrodes in Fig. 4 is calculated as 554 nm, 121 nm, 62 nm, and 34 nm, corresponding to the second, third, fourth and fifth deposition of the electrophoretic paint for an etched platinum wire, respectively.

Nanoelectrode papers generally refer to the effective or apparent radius (r_{eff}, r_{app}) of the nanoelectrode, since there is an assumption about the actual shape and the mode of diffusion governing transport to that electrode. Recently, Arrigan in his review paper dealing with the topic of the nanoelectrodes summarizes some of the steady-state voltammetric characterization of nanoelectrodes and the parameters of the electrode obtained from that analysis [16]. As can be seen, many electrodes are characterized by the hemisphere electrode model, justified on the basis that the etching/coating procedures used produce cone electrodes which can be approximated by a hemisphere [21–24].

Estimates of electrode radius based on Eq. (3) assume a hemispherical geometry of the electrode and pure diffusional transport of the electroactive species in the solution; thus the values of r_{eff} quoted in this paper are only the apparent or effective electroactive radii instead of the real electrode size. The real geometry of the electrodes may more likely be cone or hemispheroid. In addition, when the electrode size approaches values of molecular dimensions and/or the length of the electrical double layer, it is questionable whether the traditional transport and kinetic theories are an adequate description of the voltammetric behavior of such electrodes [25]. It has been generally realized that voltammetric analysis for such small electrodes may give considerable systematic errors in the determination of electron-transfer kinetics in the absence of reliable geometric information about the electrodes and an accurate description of the transport of electroactive species [26,27].

Szabo deals with the influence of insulation geometry on the limiting current at microelectrodes, and indicates that as long as the radius of the insulation is greater than twice the radius of the electrode, the infinite plane model is a useful approximation for analyzing experimental results [28].

Watkins et al. estimated the error that results from use of Eq. (3) by employing more sophisticated mathematical predictions of the current, found in the literature, for different electrode geometries [29–31]. They estimate the height of the hemispheroid by the TEM images and compute i_{lim} slightly smaller that the electrochemical experimental value [24]. The electrodes here have diffusion from behind the plane of the electrode, and therefore, the constant 2π will be larger and the estimates off a little.

Woo et al. showed an interesting switch from hemisphere to inlaid disc behavior using their additional etching procedure to remove the protruding cone [32]. It should be noted that the voltammetric properties of nanoelectrodes agree with classical diffusion theory for nanoelectrodes of effective radii >10 nm; below this limit, there is a deviation from theory. However, the microscale models have still been applied for the estimation of extremely small electrode radii, substantially less than 10 nm [16].

Of course, it is unlikely that any simple ideal geometry used in mathematical modeling will precisely describe electrodes of nanometer dimensions, as the shapes of the electrodes are difficult to control at these length scales with currently known methods. On the basis of the above comparisons, we conclude that the current is insufficiently sensitive

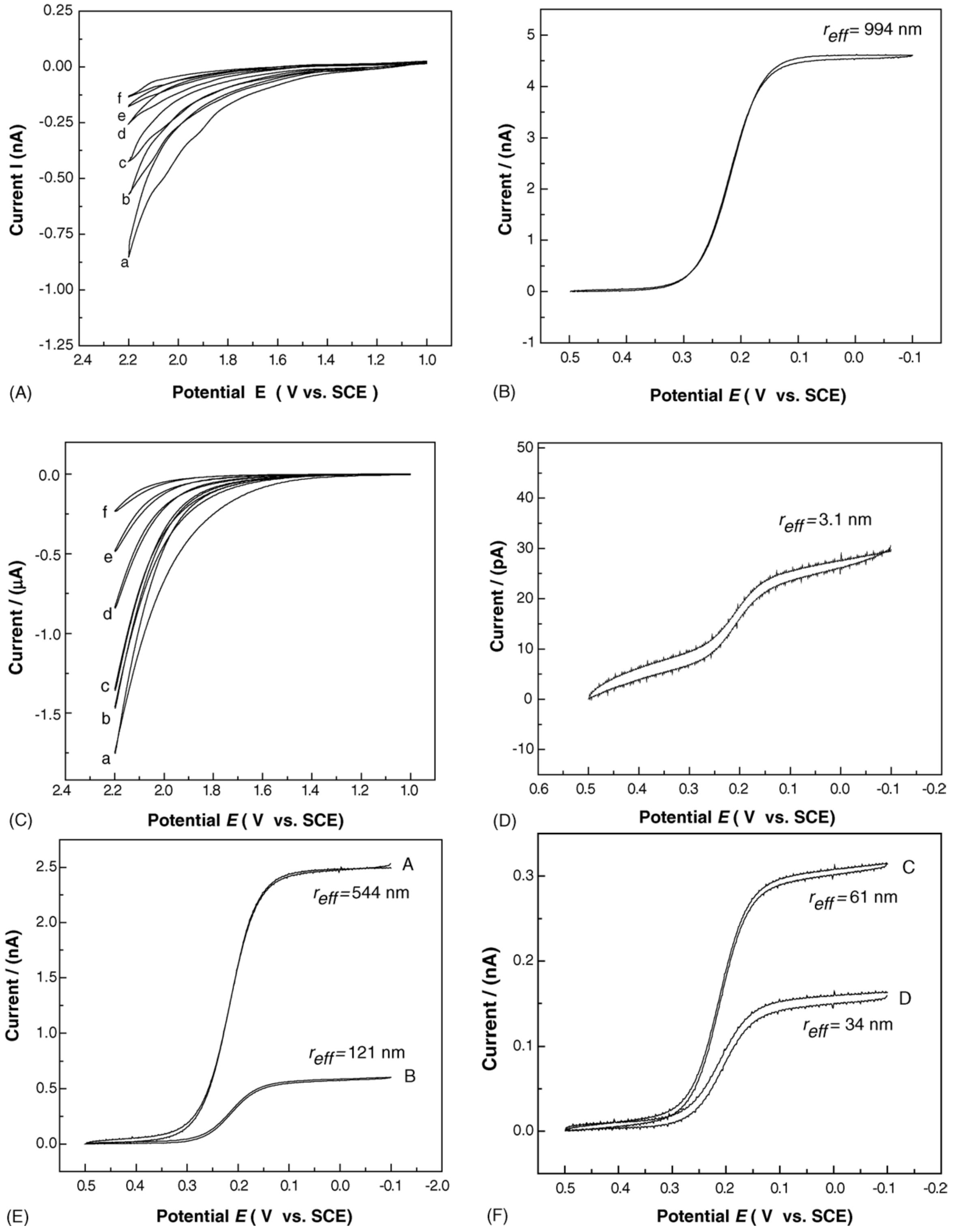

Fig. 4. The cycle voltammetric deposition of the etched electrode in the electrophoretic paint and the cycling voltammograms of the nanoelectrodes in 0.01 mol/L $K_3Fe(CN)_6$ solution containing 0.5 mol/L KCl. (A) The sixth deposition, (a)–(f) are the first, second, third, fifth, tenth, and twentieth cycle, respectively. (B) The steady-state voltammograms after the first deposition. (C) The first deposition, (a)–(f) are the first, second, third, fifth, tenth, and twentieth cycle, respectively. (D) The steady-state voltammograms after the sixth deposition. Scan rate 5 mV/s. The steady-state voltammograms of the nanoelectrodes in 0.01 mol/L $K_3Fe(CN)_6$ containing 0.5 mol/L KCl. The effective radii of the electrodes calculated from the limited currents are as follows: A–D: 544 nm, 121 nm, 62 nm and 34 nm corresponding to the second, third, fourth and fifth deposition of the electrophoretic paint for an etched platinum wire, respectively. A saturated calomel electrode was served as the reference electrode and a platinum plate was served as the auxiliary electrode. The scan rate was 5 mV/s.

Table 1
The $E_{1/2}$, $|E_{3/4} - E_{1/4}|$ and the standard rate constant k^o of different sized platinum electrodes in the 0.01 mol/L $K_3Fe(CN)_6$ and 0.5 mol/L KCl solution

r (nm)	$E_{1/2}$ (V)	$\|E_{3/4} - E_{1/4}\|$ (V)	k^o (cm/s)
3.1	0.208	0.070	8.1
10	0.208	0.068	5.8
34	0.210	0.064	3.8
41	0.211	0.063	4.2
62	0.212	0.063	2.1
81	0.213	0.062	2.9
121	0.214	0.061	1.2
544	0.217	0.061	0.7
780	0.218	0.060	*a*
994	0.221	0.059	*a*

a, Reversible reaction (no kinetic parameter can be extracted).

to allow subtle differences in geometry to be determined by voltammetric measurements [23].

According to the characterization of ultramicroelectrodes for a reversible system, the Tomes Criterion states that $|E_{3/4} - E_{1/4}|$, the potential difference between the quartile potentials, corresponding to the electrode potentials where the current is equal to 1/4 and 3/4 of the limiting value, respectively, should be $56.4/n$ mV at 298 K, where n is the number of electrons transferred during the electrochemical process [33]. The potential difference of the different-sized nanoelectrodes from 59 mV to 70 mV is shown in Table 1. With the decrease of the effective radius, the potential difference of $|E_{3/4} - E_{1/4}|$ tends to increase, and the half potentials $E_{1/2}$ tend to decrease ($E_{1/2}$ is defined as the potential where the voltammetric current equals half of the diffusion-limited value, i.e., $i = 0.5i_{\mathrm{lim}}$). This result coincides with the report of [13]. But the reversibility of the electrodes made in this work is better than that in [13] where the potential difference is in the range 61–80 mV. Figs. 3 and 4 also shows that the voltammograms of the redox of $K_3Fe(CN)_6$ become worse as the size of the electrodes decreases. It means that the reversibility of this process becomes worse with an increase of the mass transport rate with smaller electrodes [14]. Using the approach developed by Mirkin and Bard [34] the kinetic parameters can be obtained and are listed in Table 1. A number of voltammograms obtained at radii of 3.1–544 nm electrodes yield values of the standard rate constant of k^o ranged from 8.1 cm/s to 0.7 cm/s.

3.5. *Infiltrativity and sensitivity for the nanometer-sized electrodes*

When the electrode of 3.1 nm was submersed in 0.01 mol/L $K_3Fe(CN)_6$ solution containing 0.5 mol/L KCl for 3 h and the steady-state voltammetry was carried out repeatedly for nine times, the average limit current was 13.1 pA with an R.S.D. of 4.5%. With the same electrode and under above conditions, the limit current only increased 12% after 2 weeks indicating that insulation of the electrophoretic paint and the sensitivity of the nanometer-sized electrodes was reliable.

4. Conclusions

This paper reports a new and simple method for fabricating controllable insulated nanometer-sized platinum electrodes is presented. Electrochemical etching of platinum wire is employed, and then a repeated process of cycle voltammetric deposition of electrophoretic paint and heat curing for shrink film follows which effectively controls the size of the nanoelectrodes, which is different from previous DC electrolysis deposition. This technique allows complete insulation of the whole body of the etched platinum wire, except for the very tip with the shrink film during heat curing of the film, leaving an electrochemical active area with effective diameters of nanometers. The process overcomes the pinhole formation resulting from the electrophoretic paint deposition process. The size of the platinum electrodes and the thickness of the deposed paint for insulation can be properly controlled and reproduced. The fabricated electrodes show ideal steady-state voltammetric behaviors from which the effective areas of the nanoelectrodes are measured. The effective radius of the prepared nanoelectrodes ranges from 3.1 nm to hundreds of nanometers.

Acknowledgments

This work was supported by the National Natural Science Foundation of China (20375034), the Jiangsu Province Natural Science Foundation (no. BK2002045) and the Natural Science Foundation of Jiangsu Provincial Education Department (no. 02KJB150013).

References

[1] R.M. Wightman, L.J. May, A.C. Michael, Anal. Chem. 60 (1988) 769A.
[2] E.L. Ciolkowski, C.B. Rooper, J.A. Jankowski, J. Am. Chem. Soc. 114 (1992) 2815.
[3] R.H. Chow, R.L. Von, E. Near, Nature 356 (1992) 60.
[4] L.M. Moretto, N. Pepe, P. Ugo, Talanta 62 (2004) 1055.
[5] G. Chen, L.Y. Zhang, J. Wang, Talanta 64 (2004) 1018.
[6] Y. Shao, M.V. Mirkin, Anal. Chem. 69 (1997) 1627.
[7] J.J. Watkins, H.S. White, Langmuir 20 (2004) 5474.
[8] S. Hrapovic, J.H.T. Luong, Anal. Chem. 75 (2003) 2976.
[9] J. Chen, K. Aoki, Electrochem. Commun. 4 (2002) 24.
[10] C. Lee, C.J. Miller, A.J. Bard, Anal. Chem. 63 (1991) 78.
[11] R.B. Morris, D.J. Franta, H.S. White, J. Phys. Chem. 91 (1987) 3559.
[12] C.J. Slevin, N.J. Gray, J.V. Macpherson, M.A. Webb, P.R. Unwin, Electrochem. Commun. 1 (1999) 282.
[13] J.J. Watkins, J.Y. Chen, H.S. White, Anal. Chem. 75 (2003) 3962.
[14] P. Sun, Z. Zhang, J. Guo, Y. Shao, Anal. Chem. 73 (2001) 5346.
[15] J.L. Conyers, H.S. White, Anal. Chem. 72 (2000) 4441.
[16] D.W.M. Arrigan, Analyst 129 (2004) 1157.
[17] C.E. Bach, R.J. Nichols, W. Beckmann, H. Meyer, A. Schulte, O. Besenhard, P.D. Jannakoudakis, J. Electrochem. Soc. 140 (1993) 1281.
[18] C.G. Zoski, Electroanalysis 14 (2002) 1041.

[19] M.I. Montenegro, M.A. Queiros, J.L. Daschbach, Microelectrodes: Theory and Applications, Kluwer Academic Press, Dordrecht, 1991, p. 259.

[20] K.T. Kawagoe, J.A. Jankowski, R.M. Wightman, Anal. Chem. 63 (1991) 1589.

[21] C.J. Slevin, N.J. Gray, J.V. Macpherson, M.A. Webb, P.R. Unwin, Electrochem. Commun. 1 (1999) 282.

[22] N.J. Gray, P.R. Unwin, Analyst 125 (2000) 889.

[23] J.J. Watkins, J.Y. Chen, H.S. White, H.D. Abruna, E. Maisonhaute, C. Amatore, Anal. Chem. 75 (2003) 3962.

[24] C.P. Smith, H.S. White, Anal. Chem. 65 (1993) 3343.

[25] S.L. Chen, A. Kucernak, J. Phys. Chem. B 106 (2002) 9396.

[26] A.S. Baranski, J. Electroanal. Chem. 307 (1991) 287.

[27] K.B. Oldham, Anal. Chem. 64 (1992) 646.

[28] D. Shoup, A. Szabo, J. Electroanal. Chem. 160 (1984) 27.

[29] Y. Fang, J. Leddy, Anal. Chem. 67 (1995) 1259.

[30] J.C. Myland, K.B. Oldham, J. Electroanal. Chem. 288 (1990) 1.

[31] C.G. Zoski, M.V. Mirkin, Anal. Chem. 74 (2002) 1986.

[32] D.H. Woo, H. Kang, S.M. Park, Anal. Chem. 75 (2003) 6732.

[33] A.J. Bard, L.R. Faulkner, Electrochemical Methods Fundamentals and Applications, John Wiley, New York, 2001, p. 202.

[34] M.M. Mirkin, A.J. Bard, Anal. Chem. 64 (1992) 2293.